Supplementary Materials

Key physical wood properties in termite foraging decisions

Sebastian Oberst[1], Joseph C.S. Lai[2], Theodore A. Evans[3]

[1] *Centre for Audio, Acoustics and Vibrations, Faculty of Engineering and IT, University of Technology Sydney, Sydney, NSW 2040, Australia*
[2] *Acoustics & Vibration Unit, School of Engineering and Information Technology, University of New South Wales, Canberra, ACT 2600, Australia.*
[3] *School of Animal Biology, The University of Western Australia, Perth, WA 6009, Australia*

Measurements

S1 Geometry and weight measurements.

Basic quantities, such as the geometry and the (dry or moist) weight of the veneer discs were taken initially. The average veneer discs' thicknesses (every 30°) and diameters (every 120°) were based on three measurements using a vernier calliper (Kincrome©, ±0.01 mm uncertainty), see figure S1.1. For humidification each veneer disc was placed in an environmental chamber (ACS© Challenge 600, Massa Martana, Italy, figure S1.2*a*, 80% relative humidity, 28 °C) for more than eight hours. The discs' weight was determined to four significant digits (AEA 250 g, Adam Equipment Co Ltd, Milton Keynes, UK, uncertainty 0.8 ± 0.5 mg, figure S1.2*b*). Then the veneer discs were oven-dried at 105 °C for about eight hours (type XU490 France Etuves, 4kW) and cooled down via vacuum desiccator (TED Pella©, dry-seal, with silica gel, VWR, BDH, Prolabo "Chameleon C 1-3mm", figure S1.2*c*).

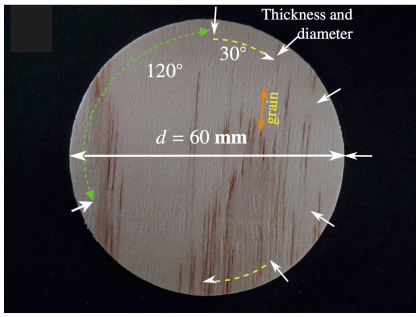

Figure S1.1. Diameter and thickness measurements. Photograph of a veneer disc showing the measuring procedure to obtain a veneer disc's thickness (every 30°) and its diameter, measured every 120°.

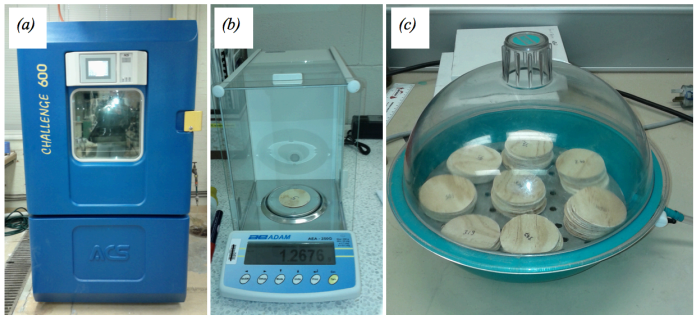

Figure S1.2. Dry and moist weight measurements of the veneer discs. *(a)*, The veneer discs are humidified using an environmental chamber and *(b)*, then weighted, followed by being oven-dried; *(c)*, then the veneer discs needed to cool down using a vacuum desiccator before being re-weighted.

S2 Light intensity measurements

Apart from geometry and weight, the colouration of the veneer discs was determined since the colour of the wood indicates different palatability, nutrition or mechanical strength [1]. All pixel intensities of all veneer discs were ranked and plotted as line graph. Intensity counts of less than fifty were assumed to belong to the background as shown in figure S2.1. Veneer pixel intensities below 125 represent late wood, and values greater than 125 indicate a higher early wood content. Figure S2.2 illustrates the pixel intensity distributions of the black background and a veneer disc with less (**LB**) and another one with more early wood (**UB**). The insert of Fig S2.2 gives only the veneer discs' intensity distributions: both are bi-modal with one peak belonging to the dark the other belonging to the lighter coloured surface parts.

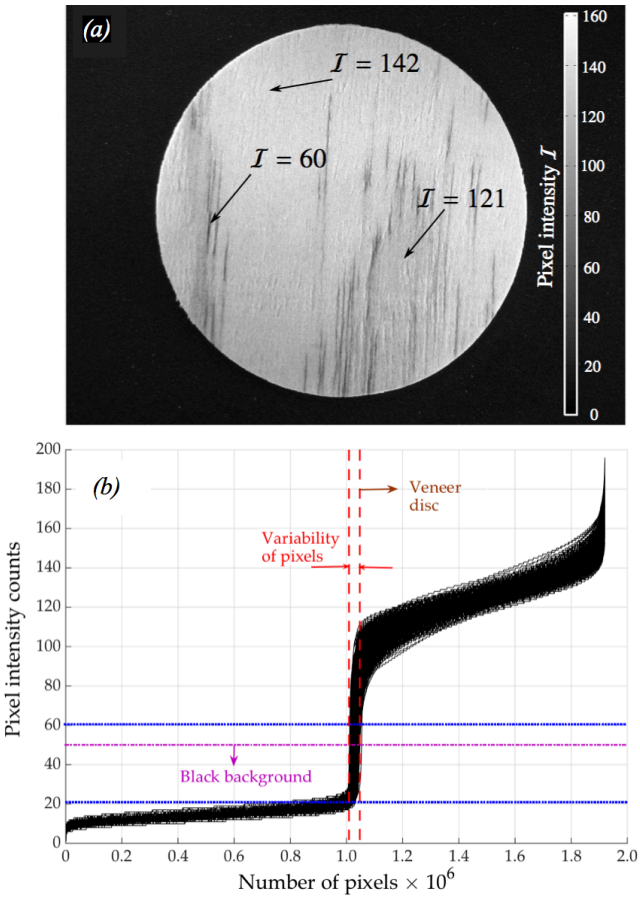

Figure S2.1. Process of determining intensity distributions.
(a), Black and white version of a figure S1.1: the intensity values are proportional to the late wood (I = 60 to 125) and the early wood (I = 142) content. *(b)*, overview of intensities of 250 veneer discs: every pixel below an intensity count of fifty was assumed to be part of the background; the measurement error was based on the variability of the pixels and was assumed to be 1.5 %, blue horizontal lines represent

*Author for correspondence (sebastian.oberst@uts.edu.au)
†Present address: Centre for Audio, Acoustics and Vibrations, Faculty of Engineering and Information Technology, University of Technology Sydney, NSW 2040, Australia

The veneer disc area could also be calculated using the photos pixel intensity and was on average $\mu \pm \sigma$: 2,827.4 ± 19.8 mm^2 with the veneer discs' thickness t being on average $\mu \pm \sigma$ = 0.922 ± 0.0541 mm (with an estimated volume of $\mu \pm \sigma$: 2,608.7 ± 153.6 mm^3). The area as well as the thickness was both weakly positive ($\rho_{5,6}$= 0.08, $\mathcal{I}_{5,6} = 0.15$, Table 1) or moderately negative correlated ($\rho_{4,6}$ = - 0.41, $\mathcal{I}_{5,6} = 0.20$) to the wood's density estimate. The area of the veneer disc is calculated over digital photography (figure S1.1) which correlated perfectly with the measured area with a near zero deviation (-1.65E-16 ± 0.007).

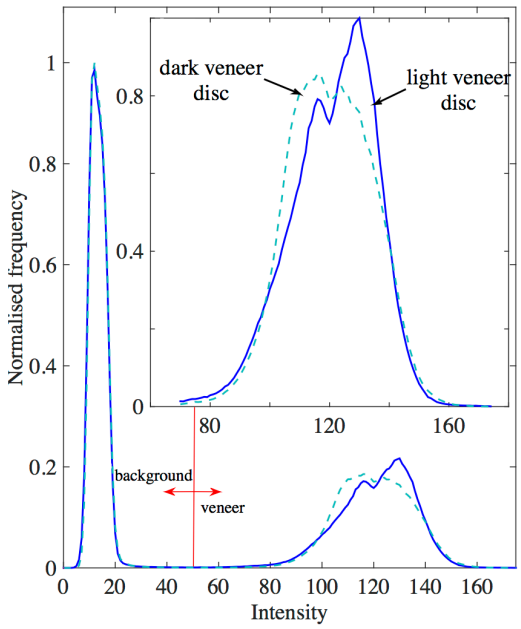

Figure S2.2. Example of intensity distributions of a lighter and a darker veneer disc. Excluding all pixel intensities below fifty provides bi-modal distributions of the two veneer discs alone (see insert): the lower peak accounting for the late wood content, the higher peak accounts for the early wood content.

S3 Generation of Histograms and subdivision into partitions

For each of the identified q key material properties, normalised histograms were created. Smoothed Epanechnikov kernels estimated the underlying theoretical continuous distributions [2]. These continuous univariate distributions were then partitioned into subsets: the first subset comprised veneer discs in the *extreme band partitions* with the lower bound (LB) and the upper bound (UB) having values respectively smaller and greater than the uni-variate distributions' mean (μ) plus/minus its standard deviation (σ) (cf. figure S3.1). All remaining discs were collected in a second subset, the *centre band partition*, which was itself divided into LB and UB samples with all key material properties being rather close to their average values.

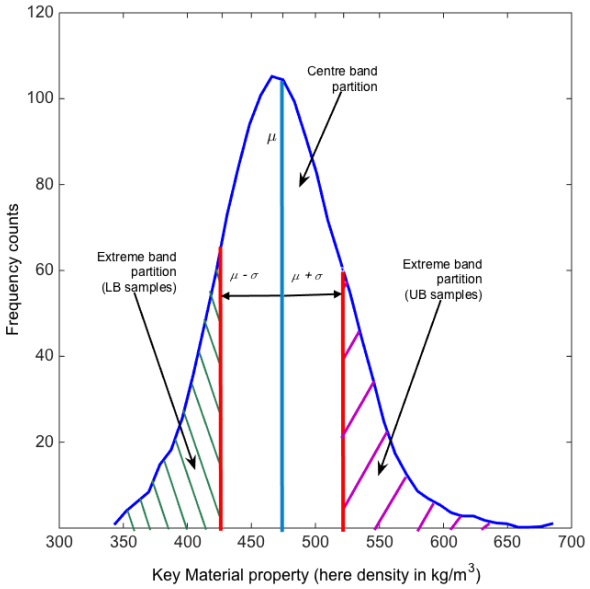

Figure S3.1. Principle of partitioning univariate distributions. Exemplified are the centre band partition bounded by the threshold values mean ± standard deviation (μ ± σ), as well as the extreme band partitions lower bound (**LB**) and upper bound (**UB**) for the key material density.

S4 Setup of termite boxes

The containers (figure 2) were equipped with two randomly chosen veneer discs to promote building activity underneath the food-choice, and locked with a lid (figure S4.1*a*,*b*) and wrapped with aluminium foil (figure S4.1*c*). Only those insect boxes in which termites started building small mounds equally on both sides with height differences less than three millimetres (measured with vernier depth rod) were used for bioassays (figure S4.1*d*).

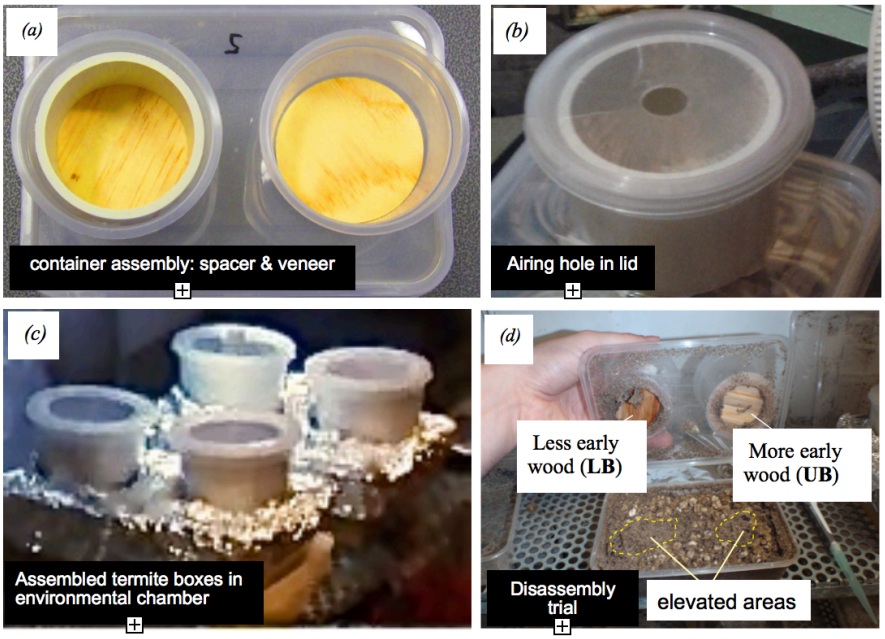

Figure S4.1. The setup of the experiments and their disassembly. *(a)*, lid of the termite box with PVC spacer (left) to push down the veneer disc; *(b)*, the PVC is pushed down by the lid with air hole to prevent the development of fungi; *(c)*, setup of termite boxes in the environmental chamber; and *(d)*, disassembled box showing one choice of more late wood **(LB)** and one which as a greater early wood content **(UB)** respectively; elevated areas of soil/clay of higher insect activity are circled.

S5 Key material parameter distributions

To reduce the number of variables, the linear and nonlinear correlations were calculated (table S5.1) using Pearson's correlation coefficient (exemplified in figure S5.1 for increasing number of samples).

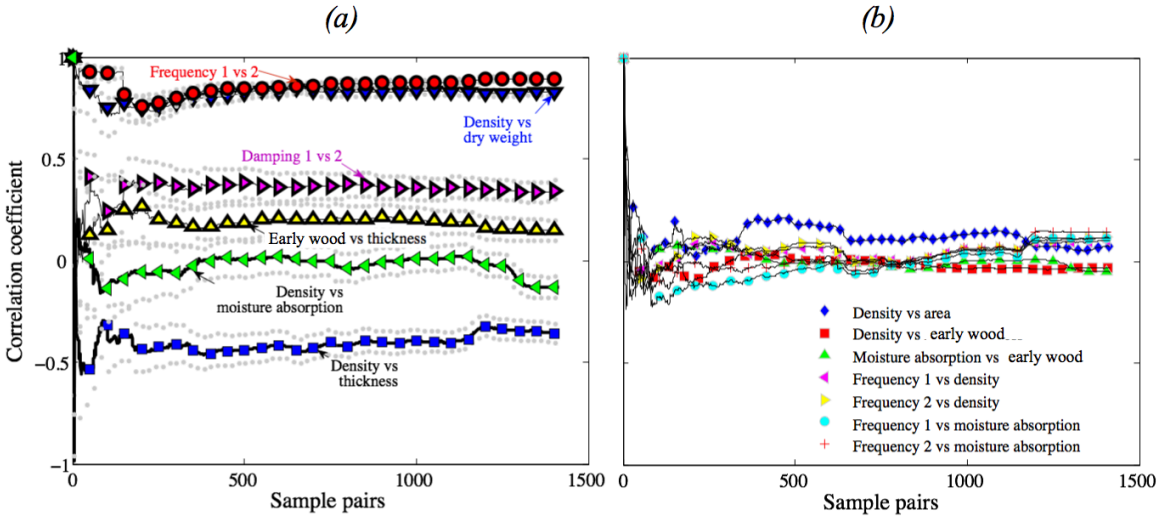

Figure S5.1. Convergence of the Pearson correlation coefficient for some extracted material parameters. *(a)*, higher values of correlation (with confidence bounds); *(b)*, lower values of correlation (for the sake of clarity without confidence bounds).

Table S5.1. **Linear and nonlinear correlation study.:** Pearson correlation coefficient ρ_{ij} (top, normal font) and normalised average cross-mutual information $\mathcal{I}_{i,j}$ (bottom, italic font) for all property vectors $\boldsymbol{X_i} := \boldsymbol{Xi}$ *with* $\in \{1, 2, \ldots, 17\}$, 1,417 veneer discs in total (see accompanying Excel sheet SI). A bold, red entry indicates strong correlation (greater or smaller than 0.64); bold, green entries highlight moderate correlation (values between ± [0.2, 0.64]); values between ±0.2 indicate a weak association

P_{ij} / $\mathcal{I}_{i,j}$		X1	X2	X3	X4	X5	X6	X7	X8	X9	X10	X11	X12	X13	X14	X15	X16	X17
Dr.y weight	X1	*	**1.0**	-0.8	**0.2**	0.1	**0.8**	-0.3	0.1	-0.7	0.0	0.1	0.1	-0.3	-0.3	0.0	-0.2	-0.2
			0.7	*0.1*	*0.1*	*0.1*	***0.2***	*0.1*	*0.1*	*0.0*	*0.1*	*0.1*	*0.1*	*0.1*	*0.1*	*0.1*	*0.1*	*0.0*
Moist weight	X2		*	0.0	**0.2**	0.1	**0.8**	-0.4	0.1	-0.8	0.0	0.1	0.1	-0.3	-0.3	0.0	-0.2	-0.3
				0.1	*0.1*	*0.1*	***0.2***	*0.1*	*0.1*	*0.0*	*0.1*	*0.1*	*0.1*	*0.1*	*0.1*	*0.0*	*0.1*	*0.0*
Humidity, $m_{RH}=x_2$	X3			*	0.0	0.1	-0.3	-0.4	0.1	-0.5	0.0	-0.1	-0.0	-0.2	0.0	0.0	0.0	-0.7
					0.1	*0.1*	*0.1*	*0.1*	*0.1*	*0.0*	*0.1*	*0.1*	*0.1*	***0.3***	***0.2***	*0.1*	*0.1*	***0.2***
Thickness	X4				*	-0.3	-0.3	0.0	-0.3	-0.0	0.1	0.0	0.0	-0.1	0.0	0.0	0.0	-0.4
						0.2	*0.2*	*0.1*	*0.2*	*0.1*	*0.2*	*0.2*	*0.1*	*0.1*	*0.1*	*0.0*	*0.1*	***0.2***
Area	X5					*	0.0	-1.0	-0.5	0.0	0.0	0.0	0.0	-0.3	-0.1	0.0	0.0	-0.1
							0.1	***0.8***	***1.0***	*0.0*	*0.1*	*0.1*	*0.1*	*0.1*	*0.1*	*0.2*	*0.0*	*0.1*
Density, $\rho=x_1$	X6						*	-0.8	0.0	0.0	-0.3	0.1	0.1	-0.2	-0.6	0.0	0.0	***0.2***
								0.1	*0.1*	*0.0*	*0.1*	*0.1*	*0.1*	*0.1*	*0.1*	*0.1*	*0.1*	*0.1*
Black area	X7							*	-0.0	0.0	-0.3	-0.5	-0.5	0.0	0.0	-0.2	0.0	0.1
									0.8	*0.0*	*0.1*	*0.1*	*0.1*	*0.1*	*0.1*	*0.0*	*0.1*	*0.1*
Bright area	X8								*	-0.5	0.0	0.0	0.0	-0.3	-0.1	0.0	0.0	-0.1
										0.0	*0.1*	*0.1*	*0.1*	*0.1*	*0.1*	*0.0*	*0.1*	*0.1*
Intensity	X9									*	-0.9	0.1	0.1	0.0	-0.1	-0.1	-0.2	0.2
											0.3	*0.1*	*0.1*	*0.1*	*0.1*	*0.1*	*0.1*	*0.1*
Early wood $l=x_3$	X10										*	-0.3	-0.2	-0.3	-0.5	0.0	-0.3	-0.5
												0.1	*0.1*	*0.1*	*0.1*	*0.1*	*0.1*	*0.1*
Frequency $f_1=x_4$	X11											*	-0.8	-0.3	-0.1	-0.9	-0.3	-0.1
													0.3	*0.1*	*0.1*	*0.0*	*0.0*	*0.1*
Frequency f_2	X12												*	-0.3	-0.2	-0.7	-0.2	-0.1
														0.1	*0.1*	*0.1*	*0.1*	*0.1*
Damping, $\xi_1=x_5$	X13													*	-0.3	-0.7	-0.4	-0.0
															0.1	***0.2***	*0.1*	*0.0*
Damping ξ_1	X14														*	-0.7	-0.5	-0.6
																0.2	***0.2***	*0.1*
Amplitude 1	X15															*	-0.3	-0.0
																	0.6	***0.3***
Amplitude 2	X16																*	-0.0
																		0.4
Sheet membership	X17																	*

Five key material properties were extracted, which were either weakly or not at all correlated to each other. This weak linear correlation is visualised using scatter plots and histograms of their normalised values are formed (figure S5.2).

The histograms were then smoothed and fitted to an analytical continuous distribution using Epanechnikov kernels to obtain an estimate of the underlying continuous distribution (figure S5.3); each of the distributions was divided into a lower bound, a centre band and an upper bound partition (see figure S3.1).

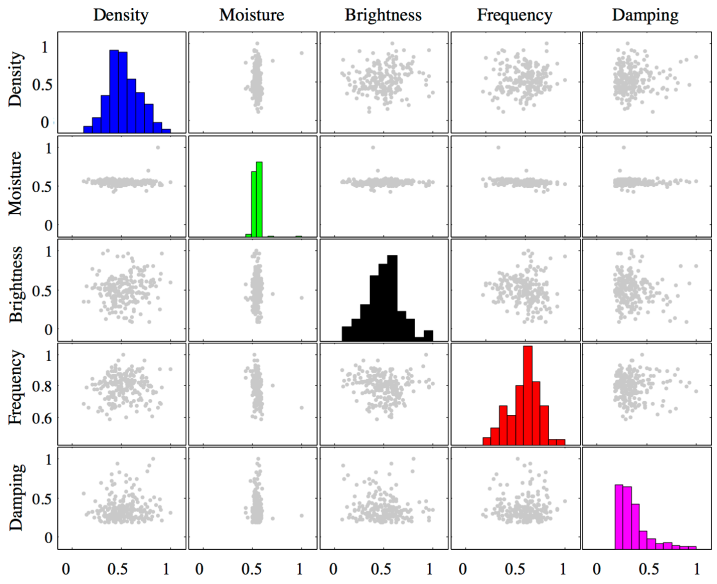

Figure S5.2. Scatter plots and histograms of key material properties. The scatter plot/ histogram matrix visualizes the results of the correlation study for the five key material properties and indicates weak or no correlation

The results of the correlation analysis between the 17 measured variables for *P. radiata* veneer discs considered in table S5.1 were similar for both the Pearson correlation coefficient P_{ij} and the averaged cross-mutual information $\mathcal{I}_{i,j}$ and converged with increasing number of correlated pairs (cf. P_{ij}, figure S4.1). Both the dry weight and the density were strongly linearly correlated with $P_{1,6}$= 0.83 and moderately correlated with $\mathcal{I}_{1,6} = 0.27$. The density ρ ($\mu \pm \sigma$: 474.58 ± 47.42 kgm^{-3}) was selected as a key material property x_1 rather than the veneer disc's dry weight, which was on average 1.235 ± 0.118 g. As termites show an affinity to moisture the ability of veneer discs to absorb humidity from the air (12.19 ± 0.88 %), was chosen as the second key property (x_2 − humidity absorption m_{RH}), which was only weakly correlated to other variables (highest $P_{3,17} = -0.17$). However, x_2 showed a moderate nonlinear correlation to the damping ratios ($P_{3,13} = -0.03, \mathcal{I}_{3,13} = 0.35$; $P_{3,14} = 0.01, \mathcal{I}_{3,14} = 0.25$). The veneer disc's mode skewness of pixel intensity distributions I indicative of the early wood content (average -0.0851± 0.3392) was selected as the third key material property x_3. The vibration magnitudes were on average A_1= −50.98 ± 24.15 and A_2= −97.47 ± 36.33 dB re 1 ms^{-1} ($P_{15,16} = 0.31, \mathcal{I}_{15,16} = 0.63$) at the first two resonance frequencies of f_1 =1,476 ± 137 Hz and f_2 = 3,679 ± 327 Hz ($P_{11,12} = 0.89, \mathcal{I}_{15,16} = 0.34$); their out-of-plane mode shapes are plotted in figure S5. The average damping ratios for these two resonance frequencies were $\zeta_1 = 3.66 \pm 1.60$ % and $\zeta_2 = 2.77 \pm 1.15$ %, ($P_{13,14} = 0.35, \mathcal{I}_{13,14} = 0.17$). As expected, $\zeta_1$and ζ_2 were negatively correlated to their vibration resonance amplitudes ($P_{13,15}$= − 0.97, $\mathcal{I}_{13,15} = 0.25$ and $P_{14,16}$= −0.95, $\mathcal{I}_{14,16} = 0.21$). Since the first and second vibration modes were reasonably correlated, only the *first* vibration mode's resonance frequency f_1 ($= x_4$), and its damping ratio ζ_1 ($= x_5$) were selected as key material properties.

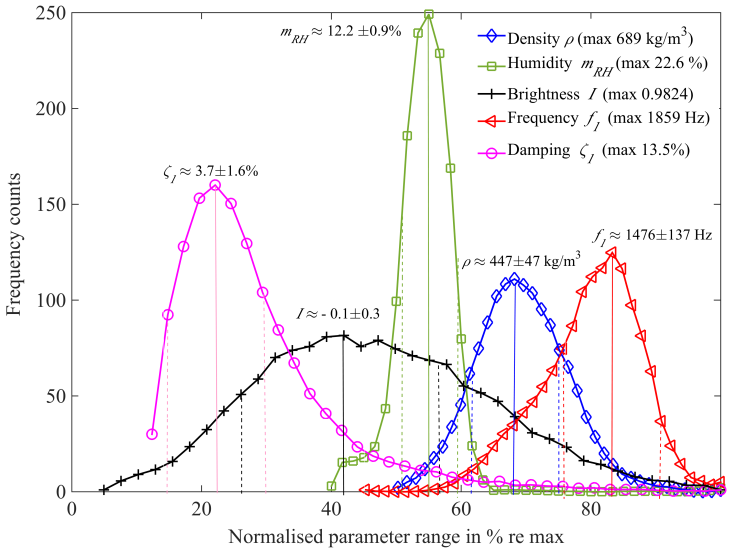

Figure S5.3. Distributions of key material properties. Estimates of continuous distributions of density, humidity absorption, early wood content, frequency and its damping relative to mean values over the parameter range (relative to its maximum value).

S6 Vibration measurements

The veneer disc's two dominant vibration modes are shown in figure S6.1. The vibration measurements were conducted using a loudspeaker as excitation source and a 2D laser scanning vibrometer PSV-400 as vibration sensor. The vibration mode shapes were characterised using the nomenclature *(m,n)* for membranes with *m* and *n* being the number of the nodal circles diameters, respectively [3,4].

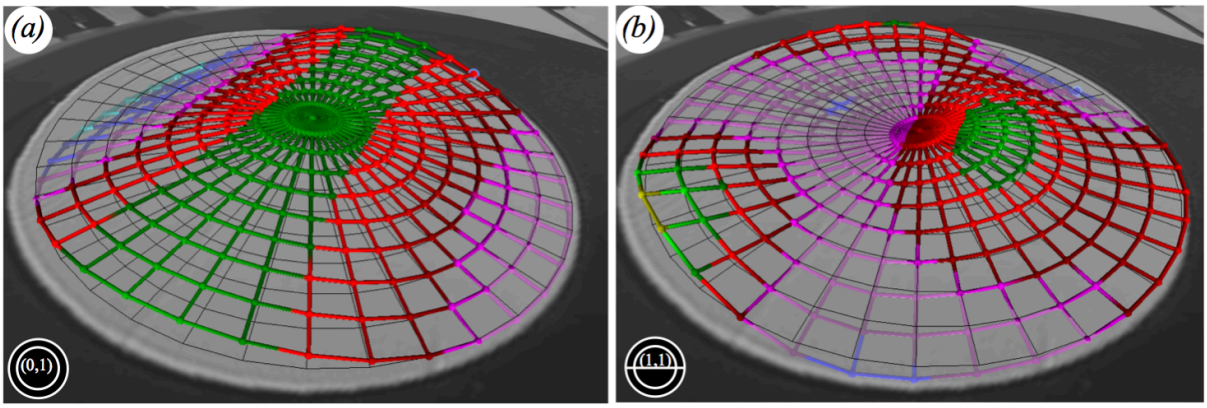

Figure S6.1. Studied vibration modes. *(a)*, at resonance f_1 with a single nodal circle (m = 1); and *(b)*, at resonance f_2 with a nodal diameter and nodal circle ($m = n$ = 1); 361 measurement points in total.

Owing to the influence of the grain and the resulting stiffness, the mode shapes were not as clear as those, which could be found for a homogeneous material. Therefore, instead of bulging out only in the veneer's centre, both mode shapes show some form of bending (figure S6.1) and e.g. the second mode (m,n) = (1,1) was visibly influenced by the (m,n) = (0,3) mode.

S7 Clustering and pairing

Figure S7.1 depicts the results of the fuzzy *c*-means clustering algorithm [5] applied to three quantities of the normalised densities' **UB** partition: frequency, moisture and damping. A plot of the cost function (CF) is inserted and indicates a decreasing curve, which reaches its minimum after about thirty iterations.
Compared to Oberst et al. [5] where the required number of iterations was 15, for the present case the algorithm had greater difficulties in distinguishing between the veneer discs; this is due to the partitioning of the distributions prior to clustering and the larger number of variables involved (five compared to three).

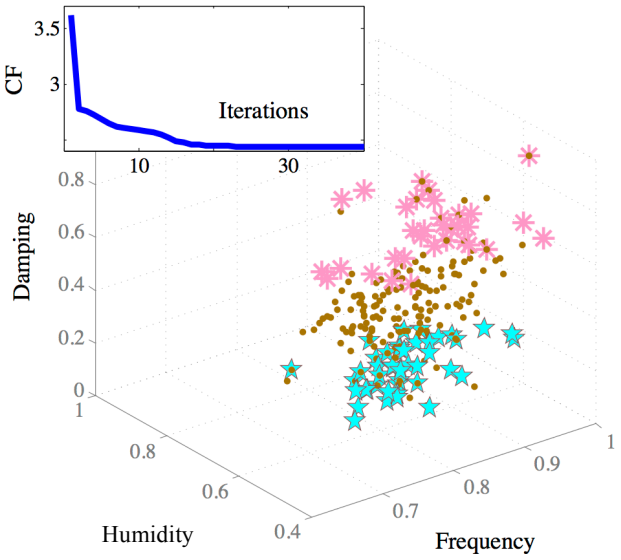

-Figure S7.1. Application of the fuzzy *c*-means clustering algorithm. Clusters of the **UB** partition (within *density*) for three other properties: damping, humidity absorption and frequency; the insert shows the cost function (CF) over iterations [5].

Within the clusters, the veneer discs formed a list with decreasing cluster membership. Then, one sample of each the **LB** and the **UB** partition were paired. Glyph plots [6] were applied to visualise the quality of the paired samples and relating the pairs to the parameter distributions. Figure S7.2*a* exemplifies the glyph plot and its variables; figure S7.2*b* provides an overview of the paired samples (**LB** and **UB** of the key material property density).

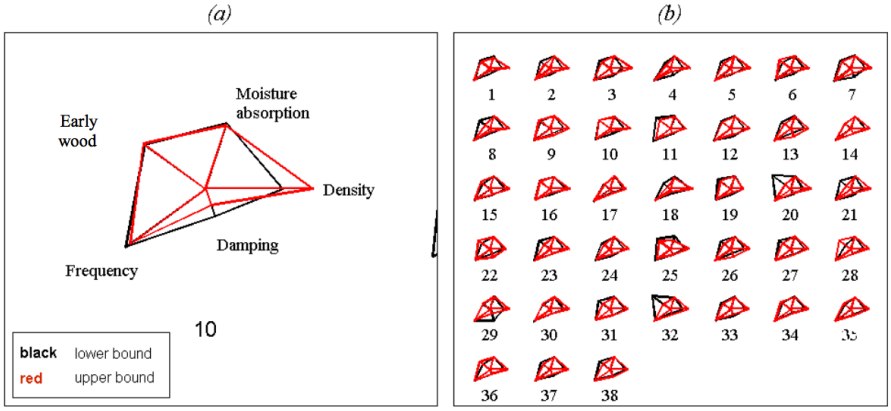

Figure S7.2. Glyph graphs to compare pairs of veneer discs. *(a)*, typical sample pair compares density as parameter for the univariate analysis for the **LB** and the **UB**; the length of the lines directed towards the centre represents each of the parameter value; *(b)*, overview of sample pairs of the key parameter density.

The minimum and maximum differences (ranges) between the veneer discs of the **LB** and the **UB** section in the extreme band partition were: for ρ about 94.7 kgm^{-3} and 294.7 kgm^{-3} with n = 35 and n = 33 samples in the **LB** and the **UB** section, respectively; for m_{RH} between 0.7 % (n = 88) and 13.6 % (n = 133); for I between 0.69 (n = 88) and 1.85 (n = 49); for f_1 between 284.4 Hz (n = 52) and 987.5 Hz (n = 24); and for ζ_1 between 2.8 % (n = 25) and 12.0 % (n = 30); the measured two dominant mode shapes are exemplified in figure S6.1.
Using the fuzzy *c*-means clustering algorithm, two or three clusters were formed within each partition (extreme or centre bands), depending on whether the sample size was (less than or equal) or > 30, respectively (figure S7.1, cf. [9]). After the application of the fuzzy *c*-means clustering algorithm, the differences of successive veneer discs in the extreme band partitions were minimised to (mean ± standard deviation) 0.4 ± 0.6 % (ρ), 0.3± 0.6 % (m_{RH}), 1.1 ± 6.4 % (I), 1.4 ± 7.9 % (f_1) and 2.6 ± 11.2 % (ζ_1) in the **LB** partitions; and to about 0.4 ± 1.0 % (ρ), 0.6 ± 4.3 % (m_{RH}), 4.4 ± 9.7 % (I), 0.3 ± 0.4 % (f_1) and 2.5 ± 15.4 % (ζ_1) in the **UB** partitions.

S8 Test of differences between colonies

Table S8.1. Colony dependency in 1-way ANOVA. No significant difference has been observed between the four colonies tested.

	Extreme bands (outer partition)			Centre band samples (inner partition)		
	# DOF	*F*-value	*p*-value	#DOF	*F*-value	*p*-value
Density	19	1.24	0.3295	21	0.64	0.6017
Moisture	19	0.88	0.4741	14	2.94	0.0804
Brightness	19	0.11	0.9525	21	1.21	0.336
Frequency	19	1.58	0.2334	13	0.45	0.7219
Damping	19	1.36	0.2918	14	1.69	0.2265

S9 Complete list of *n*-ANOVA test

Table S8.2. **5-ANOVA test results (complete).** Results of the five factorial ANOVA test for all samples (extreme- and centre-band samples) to test for interactions between the five parameters density, moisture absorption, brightness, frequency and damping; X3, X6, X10, X11 and X13 according to data table (Supplementary Materials).

	Sum squared	Mean Squared	F-value	*p* - value
Density (X6)	1.685	1.68499	4.36	0.0385
Moisture (X3)	0.7955	0.7955	2.06	0.1535
Brightness (X10)	0.1429	0.1429	0.37	0.5441
Frequency (X11)	0.1406	0.14058	0.36	0.5474
Damping (X13)	1.183	1.18301	3.06	0.0823
X6*X3	0.0389	0.0389	0.1	0.7515
X6*X10	0.7981	0.79807	2.06	0.1528
X6*X11	0.5748	0.57479	1.49	0.2246
X6*X13	0.1082	0.10823	0.28	0.5975
X3*X10	0.005	0.00504	0.01	0.9092
X3*X11	0.4573	0.45727	1.18	0.2785
X3*X13	1.0935	1.09353	2.83	0.0946
X10*X11	0.75	0.75001	1.94	0.1657
X10*X13	0.1026	0.10265	0.27	0.6071
X11*X13	0.0364	0.03639	0.09	0.7594
X6*X3*X10	2.4879	2.48791	6.44	0.0122
X6*X3*X11	0.3258	0.32583	0.84	0.36
X6*X3*X13	0.1961	0.1961	0.51	0.4774
X6*X10*X11	1.554	1.55405	4.02	0.0467
X6*X10*X13	0.0006	0.0006	0	0.9687
X6*X11*X13	0.009	0.00904	0.02	0.8786
X3*X10*X11	0.6152	0.61516	1.59	0.2091
X3*X10*X13	0.0081	0.00811	0.02	0.885
X3*X11*X13	0.0149	0.01492	0.04	0.8445
X10*X11*X13	0.547	0.54705	1.42	0.2361
X6*X3*X10*X11	0.0541	0.05407	0.14	0.7089
X6*X3*X10*X13	0.0077	0.00768	0.02	0.8881
X6*X3*X4*X13	0.5113	0.51129	1.32	0.2519
X6*X10*X11*X13	0.0597	0.05974	0.15	0.6948
X3*X10*X11*X13	0.0762	0.07618	0.20	0.6577

S10 Permutation analysis

Figure S10.1*a* provides relative frequencies for every ε calculated from the statistics of comparing permutations with each other within the sport index bet model; by bootstrapping and randomly pairing the veneer discs (case (i)), many veneer disc pairs showed negligible differences in their material properties and approach 100 % relative frequency for material differences greater than $\varepsilon = 39$ %. This means that for $\varepsilon > 39$ % many veneer discs are similar and for $\varepsilon > 92$ % almost 100 % of the veneer discs show no difference (i.e. [0 0 0 0 0] = none of the properties is dominant more than 90 %).

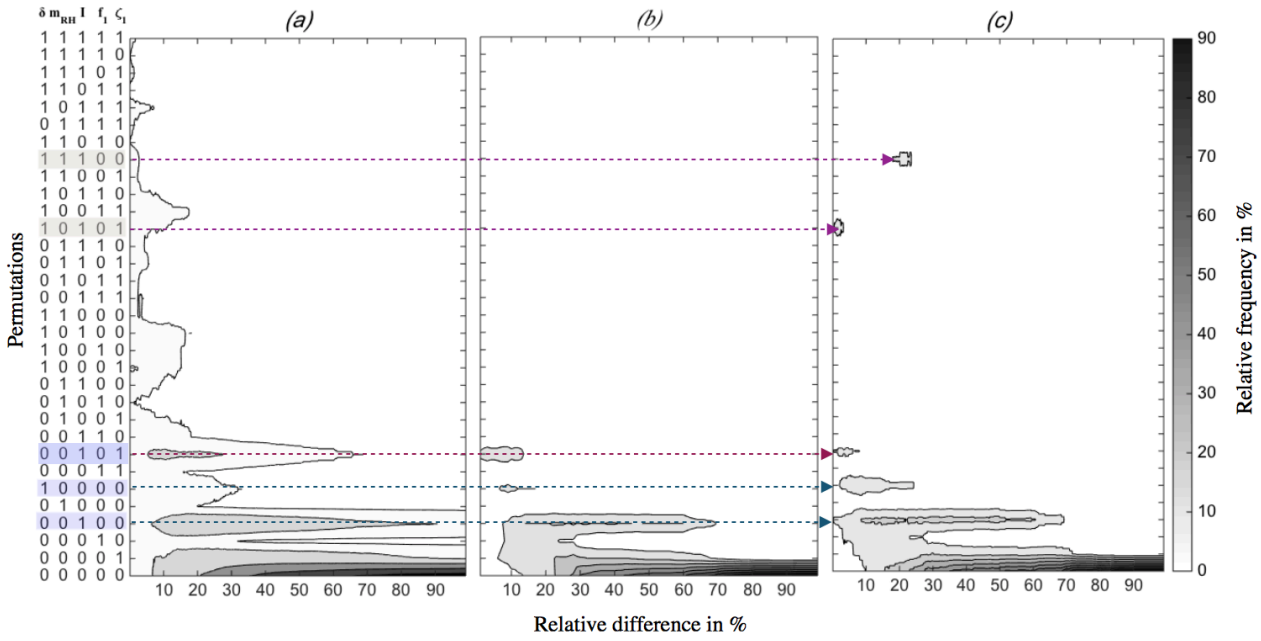

Figure S10.1. Multivariate permutation analysis. Distributions of randomly drawn sample pairs of five key material parameters: *(a)*, 10,000 samples bootstrapped with replacement from 1,417 veneer discs; *(b)*, 188 experimental sample pairs selected using them in bioassays (see Step C, figure 1) and *(c)*, results of 188 experimental sample pairs after being used in the bioassay food-choice experiment. As indicated by the horizontal arrows, termites preferred dense wood, with a greater early wood content which is humidified or highly damped; δ- density, m_{RH}- humidity, I- early wood, f_1- frequency, ζ_1- damping ratio.

The permutations [0 0 1 0 1] (i.e. the **UB** has more early wood and a higher damping ratio), [0 0 1 0 0] (UB greater early wood content) and [0 0 0 0 1] (UB with higher damping ratio) showed relative frequencies of 9 %, 22 % and 29 % and differences up to ε = 70 %, ε = 90 % and ε = 80 %. Then, the bootstrapped results of case (i) were compared to the results of the experimentally paired samples (case (ii)), figure S10.1*b*: veneer disc pairs of case (ii) represent a subset of the randomly mixed and paired veneer discs of case (i). Figure S 10.1*c* shows the results of case (iii): termites preferred a higher density [1 0 0 0 0] and with higher early wood content [0 0 1 0 0]. Further, the combinations [0 0 1 0 1], [1 0 1 0 1] and [1 1 1 0 0] show peaks indicating that termites preferred denser wood with greater early wood content, higher damping or humidity.

Figure S10.2 gives the difference in relative frequencies calculated from figure S10.1; the choice of the termites minus the relative frequencies of the food provided. Values greater than zero indicate a positive relative preference, whereas values less than zero indicate that less of this wood was eaten relative to what was provided (negative preference).

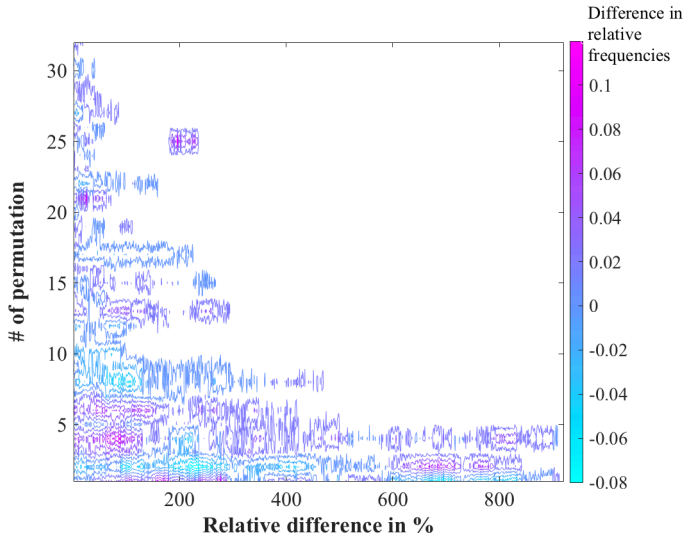

Figure S10.2. Integrated results of permutations. Number of permutation against relative difference of calculated differences in relative frequencies of termite choice (Figure S10.1*c*) minus relative frequencies of wood provided (Figure S10.1*b*).

S11 Canonical Correlations

Whether the natural distribution of wood properties was correlated with the choice of the termites, was calculated using Wilk's likelihood ratio λ and canonical correlations [6]. With λ we compared the statistical significant differences of multivariate canonical correlations with $\lambda < 0.05$ indicating correlation [2]. Canonical correlations estimate the linkage

between two sets of permutations; two vectors (directions) $\boldsymbol{\alpha}$ and $\boldsymbol{\beta}$ are determined and their covariance is maximised to determine their influence on the observed data [2]. The product of the directions $\boldsymbol{\alpha_1}, \boldsymbol{\beta_1}$ within the canonical variable scores shows a diagonal pattern in case of a strong association between **X** (the natural wood distribution) and **Y** (termites preferred choice) and a cloud of points for a weak correlation,
$\boldsymbol{\alpha_1}, \boldsymbol{\beta_1} = \max_{||\mathbf{X}\boldsymbol{\alpha}||_2=1,\, ||\mathbf{Y}\boldsymbol{\beta}||_2=1} \arg\{\mathrm{cov}\,(\mathbf{X}\boldsymbol{\alpha}, \mathbf{Y}\boldsymbol{\beta})\}$.

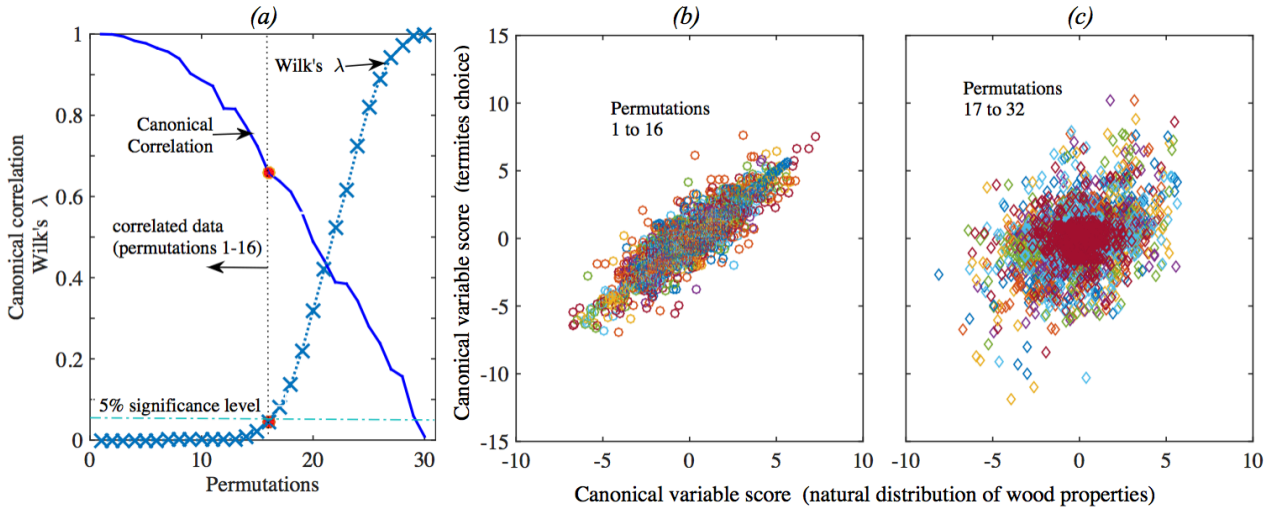

Figure S11.1. Correlation of termites' food choice with wood properties for different permutations of wood properties. *(a)*, canonical correlation coefficient and Wilk's λ of the natural distribution of wood properties (Fig S10.1*a*) against the termites' choice (Fig S10.1*c*): correlations are significant ($\lambda < 0.05$) up to the 16th permutation; *(b)*, which is also indicated by a linear relationship; whereas in *(c)*, permutations 17 to 32 form a cloud of points which indicate no correlation.

In figure S11.1*a*, below the 17th permutation (figure 10.1, permutations [0 0 … 0] to [1 1 0 0 0]) all $\boldsymbol{\lambda}$ were smaller than 0.05 and all canonical correlation coefficients comparing the natural wood property distribution (case (i)) and the termites' food preference (case (iii)) were greater than 0.65, indicating significant correlation. Plotting the canonical variable scores of the wood properties against the termite food preference score provides a linear relationship up to the 16th permutation (figure S11.1*b*); above the 16th permutation the scores are uncorrelated (figure S11.1*c*).
Comparing whole sets of permutations with the number of wood samples (resolving thereby the sensitivity axis) termites food choice shows a strong and significant correlation to those properties of wood, which are mostly available. An interpretation of these results, however, is difficult: while sample size is enough to test this the use of another distribution of wood, which strongly differs to *P. radiata* or even manufactured particle boards or structures of bamboo could be used.

References Supplementary Material

1. Csanady E, Magoss E. 2013. Mechanics of Wood Machining. Springer-Verlag, Berlin, Heidelberg.
2. Seber GAF. 1984. Multivariate Observations. Hoboken, NJ: John Wiley & Sons, Inc.
3. Fletcher NH, Rossing TD. 1998. The physics of musical instruments. Springer-Verlag New York.
4. Oberst S, Lai JCS. 2015. Pad-modes-initiated instantaneous mode instability for simple models of brake systems, Mech. Sys. Sig. Proc., 62-63, 490 - 505.
5. Oberst S, Lai JCS, Evans TA. 2014. Novel method for pairing wood samples in choice tests, PLoS One 9, e88835.
6. Martinez WL, Martinez AR. 2002. Computational Statistics Handbook with Matlab, Chapman & Hall/CRC Press Boca Raton, Florida, USA.